Black-hole ringdown as a probe of higher-curvature gravity theories

Hector O. Silva,[1] Abhirup Ghosh,[1] and Alessandra Buonanno[1,2]

[1]*Max Planck Institute for Gravitational Physics (Albert Einstein Institute), Am Mühlenberg 1, Potsdam 14476, Germany*
[2]*Department of Physics, University of Maryland, College Park, Maryland 20742, USA*

(Dated: March 30, 2022)

I. INTRODUCTION

[HS: AB will do this.]

Theory	Constraint	This work
EdGB	$\ell_{\rm GB} \leqslant 1.18$ km (GW) [1]	–
dCS	$\ell_{\rm CS} \leqslant 8.5$ km (EM+GW) [2]	$\ell_{\rm CS} \leqslant 38.7$ km
cubic EFT	–	$\ell_{\rm cEFT} \leqslant 38.2$ km
quartic EFT	$\ell_{\rm qEFT} = \ldots$ km [3]	$\ell_{\rm qEFT} \leqslant 51.3$ km

TABLE I. [HS: Mention it in the Introduction later, in a sort of 'executive summary'.]

II. OVERVIEW OF MODIFIED GRAVITY THEORIES

We briefly review the theories we consider in this paper, what the currents observational constraints are in each of them and what we know about BH QNMs in each of them.

A. scalar-Gauss-Bonnet gravity

This theory is given by the following action,

$$S_{\rm GB} = \frac{1}{16\pi}\int {\rm d}^4x\,\sqrt{-g}\left[R - \tfrac{1}{2}(\nabla\varphi)^2 + \tfrac{1}{4}\ell^2_{\rm GB} f(\varphi)\mathscr{G}\right], \quad (2.1)$$

where R is the Ricci scalar associated with the metric $g_{\alpha\beta}$ and φ is a dynamical scalar field which couples to the Gauss-Bonnet invariant $\mathscr{G}$,

$$\mathscr{G} = R^{\mu\nu\rho\sigma}R_{\mu\nu\rho\sigma} - 4R^{\mu\nu}R_{\mu\nu} + R^2, \quad (2.2)$$

with strength set by the dimensionful coupling constant $\ell_{\rm GB}$ with dimensions of length. Different subclasses of this theory are determined by the function $f(\varphi)$ and they can be classified into two classes based on the properties of their BH solutions. In the first class, the first derivative of the coupling function $f'(\varphi) = {\rm d}f/{\rm d}\varphi$ is always nonzero and BHs are known to always support (secondary) scalar hair. Examples include the shift-symmetric $f \propto \varphi$ and dilatonic $f \propto \exp(\varphi)$ couplings. In the second class, $f'(\varphi) = 0$ can vanish for some constant φ_0. In this case, one can show that theory admits the same stationary, asymptotically flat BH solution of GR and scalarized BHs [4–8]. Examples include the quadratic $f \propto \varphi^2$ [5] and Gaussian $f \propto \exp(-\varphi^2)$ [4] couplings. Here we will consider only the dilatonic theory.

BHs in both classes support monopolar scalar hair and thus, when in binaries, can source scalar dipole radiation and are therefore prone to be constrained with GWs observations of compact binaries [9, 10]. ...

The calculation of the QNMs in this theory is more complicated than in GR already for nonrotating BHs. The reason is due to the coupling between scalar field and the Gauss-Bonnet invariant, which manifests into a coupling between scalar perturbation and gravitational perturbations of polar parity ...

B. dynamical Chern-Simons gravity

This theory is given by the following action,

$$S_{\rm CS} = \frac{1}{16\pi}\int {\rm d}^4x\,\sqrt{-g}\left[R - \tfrac{1}{2}(\nabla\vartheta)^2 + \tfrac{1}{4}\ell^2_{\rm CS}\,\vartheta\,{}^*RR\right], \quad (2.3)$$

where ϑ is a pseudo-scalar field, which couples to the Pontryagin density,

$${}^*RR = {}^*R^{\mu}{}_{\nu}{}^{\rho\sigma}R^{\nu}{}_{\mu\rho\sigma}, \quad (2.4)$$

where ${}^*R^{\mu}{}_{\nu}{}^{\rho\sigma}$ is the dual of the Riemann tensor, defined as ${}^*R^{\mu}{}_{\nu}{}^{\rho\sigma} = \frac{1}{2}\epsilon^{\mu}{}_{\nu\gamma\delta}R^{\gamma\delta\rho\sigma}$, and where $\epsilon^{\mu}{}_{\nu\gamma\delta}$ is the Levi-Civita tensor. The coupling between scalar field and the Pontryagin density is set by the $\ell_{\rm CS}$ with dimensions of length.

The theory admits the Schwarzschild BH solution of GR, but predicts that spinning BHs have (secondary) scalar hair, which, unlike in scalar-Gauss-Bonnet gravity, is dipolar [11, 12]. Consequently, the leading-scalar radiation channel is quadrupolar making this theory presently unconstrained by from the GWs from the inspiral of BH binaries alone [9, 10]. However, the theory has been constrained by Ref [2] through a combination information of x-ray observations of the isolated neutron star PSR J0030+0451 [13, 14] by the NICER [15, 16] and gravitational-wave observation of the binary neutron star event GW170817 [17].

Similarly to the case of scalar-Gauss-Bonnet gravity, the perturbations of nonrotating BHs in dynamical Chern-Simons gravity also have a coupling between scalar and metric perturbations. However, the coupling is between the scalar and gravitational perturbations of axial parity [18–21].

C. Effective-field-theory of GR

This theory is given by the following action,

$$S_{\rm EFT} = \frac{1}{16\pi}\int {\rm d}^4x\,\sqrt{-g}\left[R + \sum\nolimits_{n\geqslant 2}\ell^{2n-2}L^{(2n)}\right], \quad (2.5)$$

where ℓ is some length scale, assumed to be small compares to the length scale associated with a BH, i.e., $\ell/M \ll 1$, and

$L^{(2n)}$ are corrections to the Einstein-Hilbert term action that introduce involving higher-order curvature tensors (with $2n$ metric derivatives).

More specifically, we follow Refs. [22, 23] and work up to dimension-eight operators (i.e., $n = 4$),

$$L^{(6)} = \lambda_{\rm e} R_{\mu\nu}{}^{\rho\sigma} R_{\rho\sigma}{}^{\gamma\delta} R_{\gamma\delta}{}^{\mu\nu} + \lambda_{\rm o} R_{\mu\nu}{}^{\rho\sigma} R_{\rho\sigma}{}^{\gamma\delta} \tilde{R}_{\gamma\delta}{}^{\mu\nu}, \tag{2.6a}$$

$$L^{(8)} = \varepsilon_1 C^2 + \varepsilon_2 \tilde{C}^2 + \varepsilon_3 C\tilde{C}, \tag{2.6b}$$

where $\lambda_{\rm o,e}$ and ε_i ($i = 1, 2, 3$) are dimensionless parameters.

BHs in these theories were found in Refs. [22, 24] for the dimension-six EFT and in Refs. [25] for the dimension-eight EFT.

Here we will consider $\lambda_{\rm e} = \lambda_{\rm o} = 1$ for simplicity in the cubic EFT, while in quartic, we will $\varepsilon_1 = 1$ and $\varepsilon_{1,2} = 0$. This is the same subset of the EFT's parameter space studied in [3].

III. METHODS

A. The parametrized ringdown spin expansion coefficients framework

We start by reviewing the parametrized ringdown spin expansion coefficients (ParSpec) framework introduced in Ref. [26], but following some of the notation used in Ref. [27].

A general procedure to describe deviations from the Kerr QNM frequencies $\omega_k^{\rm Kerr}$ and damping times $\tau_k^{\rm Kerr}$ is to write,

$$\omega_k = \omega_k^{\rm Kerr}\,(1 + \delta\omega_k), \tag{3.1a}$$

$$\tau_k = \tau_k^{\rm Kerr}\,(1 + \delta\tau_k), \tag{3.1b}$$

where $\delta\omega_k$ and $\delta\tau_k$ are the deformation parameters. Here we use the subscript k to represent the QNM labels $\{l, m, n\}$, where l and m are the multipole indices, and n the overtone number. This approach was adopted, e.g., in Refs. [28–30].

A caveat of parametrizations of the form (3.1), is that $\delta\omega_k$ and $\delta\tau_k$ depend, in general, on the BH's source mass and spin. Ideally, one would like to explicitly reinstate the dependence the source-frame BH mass and spin for it would (i) introduce deformation parameters which can be determined, once and for all, from a specific gravity theory, and (ii) make it easy to combine constraints from multiple source.

In the ParSpec framework this is accomplished by performing a bivariate expansion of Eq. (3.1) in the detector-frame mass and spin, namely

$$\omega_k = \frac{1}{M}\sum_{n=0}^{N_{\rm max}} \chi^n \omega_k^{(n)} \left(1 + \gamma\delta\omega_k^{(n)}\right), \tag{3.2a}$$

$$\tau_k = M\sum_{n=0}^{N_{\rm max}} \chi^n \tau_k^{(n)} \left(1 + \gamma\delta\tau_k^{(n)}\right), \tag{3.2b}$$

where M and χ are the detector-frame mass and dimensionless spin of the black hole; ω_k^n, τ_k^n are dimensionless coefficients of the spin expansion for Kerr QNMs; $\delta\omega_k^{(n)}$, $\delta\tau_k^{(n)}$ are source-independent dimensionless coefficients that characterize the corrections to the Kerr QNM at each spin-order; and finally $N_{\rm max}$ is the order of the spin expansion. All source dependence on the beyond-GR modification is encapsulated in the dimensionless parameter γ given by,

$$\gamma = \left(\frac{\ell}{M_{\rm s}}\right)^p = \left[\frac{\ell c^2 (1+z)}{GM}\right]^p, \tag{3.3}$$

which depends on the parameter ℓ, with dimensions of length (and sets the lengthscale at which beyond-GR modifications become important), and the exponent p which is related to how the beyond-GR modifications are included to the Einstein-Hilbert action. In Eq. (3.3) we made ℓ dimensionless by using the other lenghtscale associated to the remnant black hole, i.e., its source-frame mass $M_{\rm s}$, which we can also write in terms of the detector-frame mass M through the redshift z [31].

In principle, a modification to GR would also affect M and χ and the expansion should be written in terms of non-GR mass and spin, say $\bar{M}$ and $\bar{\chi}$. If we assume that the beyond-GR corrections are included perturbatively, the modifications to the BH mass and spin can be absorved into the deviations parameters $\delta\omega$ and $\delta\tau$. This means we can identify the M and χ with their *corresponding GR values*.

We remark that in the GR limit, where $\delta\omega_k^{(n)} = \delta\tau_k^{(n)} = 0$ $\forall\, n$, the series (3.2) truncated at $N_{\rm max} = 4$, reproduces with 1% accuracy the Kerr QNMs for spins $\chi \lesssim 0.7$. The values of the fitting coefficients $\omega_k^{(n)}$ and $\tau_k^{(n)}$ can be found in Ref. [26], Table I.

[HS: TODO: say that we check a posteriori if our PE runs agree with this.]

B. The parametrized waveform model

In this section we describe the waveform model used in our paper to measure properties of a BBH ringdown. As in [32, 33], we use an inspiral-(plunge)-merger-ringdown (IMR) BBH waveform model where the parameters describing the remnant object are left additionally free and estimated directly from the data.

The GW signal from a BBH merger can be determined in GR by a unique set of parameters $\boldsymbol{\theta}$, that includes the masses and spins of the two BHs, (m_1, m_2, $\vec{s}_1$, $\vec{s}_2$), the sky location determined by the luminosity distance d_L, right ascension α and declination δ, and the orientation of the binary given by the inclination and polarization angles, (ι, ψ). The set is completed by the choice of a reference time and phase, (t_0, ϕ_0). If we further assume that the spins of the individual BHs are restricted to be parallel to the orbital angular momentum, then we reduce the 6 components of spin to just 2, (χ_1, χ_2) and our entire parameter set from 15 to 11. We define some additional parameters and set some conventions that will be useful in our analysis later, namely, the totat mass $M = m_1 + m_2$, the chirp mass $\mathcal{M} = (m_1 m_2)^{3/5}/(m_1 + m_2)^{1/5}$, the asymmetric mass ratio $q = m_1/m_2$ with the convention $m_1 \geqslant m_2$; $q \geqslant 1$ and the symmetric mass ratio of the binary, $\nu = m_1 m_2/(m_1 + m_2)^2$.

The polarization of the GW signal (in the observer's frame)

are,

$$h_+(\iota,\varphi_0;t) - i h_\times(\iota,\varphi_0;t) = \sum_{l,m} {}_{-2}Y_{lm}(\iota,\varphi_0)\, h_{lm}(t)\,, \tag{3.4}$$

where ${}_{-2}Y_{lm}(\iota,\varphi_0)$ are the -2 spin-weighted spherical harmonics described by standard angular dependence indices (l,m).[1] As our baseline model, we use the computationally efficient (time-domain) multipolar waveform model for quasicircular spin-aligned BBH mergers described in [34] (henceforth referred to as SEOBNR[2]) which contains the modes, $(l,|m|) = (2,2),(2,1),(3,3),(4,4)$, and $(5,5)$ [34, 36]. The model uses an effective-one-body approach combined with a post-adiabatic solution of the equations of motion to describe the inspiral-plunge waveform, $h_{lm}^{\rm insp-plunge}$. An accurate description of the merger is incorporated through calibration with NR simulations, as described in [36], along with information for the merger and ringdown phases, from BH perturbation theory. The merger-ringdown waveform, $h_{lm}^{\rm merger-RD}$, is then stitched to inspiral-plunge waveform, $h_{lm}^{\rm insp-plunge}$ at a certain time $t = t_{lm}^{\rm match}$, as

$$h_{lm}(t) = h_{lm}^{\rm insp-plunge}\,\theta(t_{\rm match}^{lm} - t) + h_{lm}^{\rm merger-RD}\,\theta(t - t_{\rm match}^{lm})\,, \tag{3.5}$$

where $\theta(t)$ is the Heaviside step function. The merger-ringdown waveform is expressed as an exponentially damped sinusoid [34, 36, 37]

$$h_{lm}^{\rm merger\text{-}RD}(t) = \nu\,\tilde{A}_{lm}(t)\, e^{i\tilde{\phi}_{lm}(t)}\, e^{-i\sigma_{lm0}(t - t_{lm}^{\rm match})}, \tag{3.6}$$

where

$$\begin{aligned}\sigma_{lm0} &= {\rm Re}(\sigma_{lm0}) + i\,{\rm Im}(\sigma_{lm0})\,,\\ &= \omega_{lm0} - i/\tau_{lm0}\,,\end{aligned} \tag{3.7}$$

are the complex frequencies of the fundamental ($n = 0$ overtone) QNMs of the remnant BH. The frequencies ω_{lm0} and damping times τ_{lm0} of the (l,m) QNM can be read off from the real and imaginary parts of σ_{lm0} respectively. The functions $\tilde{A}_{lm}(t)$ and $\tilde{\phi}_{lm}(t)$ are defined in [36, 37].

In the SEOBNR model [34], the complex frequencies σ_{lm0} are computed by first determining the final mass and spin from estimates of the initial masses and spins through NR–fitting–formulas [38, 39] and then converting them to the complex frequencies using BH perturbation theory–inspiral analytical fits outlined in [40, 41]. Hence,

$$\omega_{lm0}^{\rm GR} = \omega_{lm0}^{\rm GR}(m_1,m_2,\chi_1,\chi_2)\,, \tag{3.8a}$$
$$\tau_{lm0}^{\rm GR} = \tau_{lm0}^{\rm GR}(m_1,m_2,\chi_1,\chi_2)\,. \tag{3.8b}$$

where $(\omega_{lm0}^{\rm GR}, \tau_{lm0}^{\rm GR})$ refer to the QNM predictions in baseline SEOBNR model. In this paper, however, we introduce a completely different expression of the QNM frequencies $(\omega_{lm0}, \tau_{lm0})$, as a series expansion on the spin of the remnant object χ_f [see Eqs. (3.2)]. For the rest of the paper, in keeping with the conventions introduced in Sec. III A, we are going to use the index k to refer to $(l,m,n=0)$ mode. Accordingly, we are going to use (ω_k,τ_k) to refer to $(\omega_{lm0},\tau_{lm0})$ respectively.

In this formalism our QNM frequencies are expressed through functions,

$$\omega_k = \omega_k(m_1,m_2,\chi_1,\chi_2,\ell,\{\delta\omega_k^{(j)}\}), \tag{3.9a}$$
$$\tau_k = \tau_k(m_1,m_2,\chi_1,\chi_2,\ell,\{\delta\tau_k^{(j)}\}), \tag{3.9b}$$

where we fixed a certain value of p, and the estimates of $(m_1, m_2, \chi_1, \chi_1)$ are used to predict the final mass and spin (M_f, χ_f) through [38, 39]. Additionally, (ω_k, τ_k) depend on the coupling constant ℓ defined in Eq. (3.3) as well as the sets, $\{\delta\omega_k^{(n)}\}$, and $\{\delta\tau_k^{(n)}\}$, where n ranges from zero to the power of spin in Eqs. (3.2) up to which we include corrections. For example, if we restrict ourselves to corrections with $n = 0$, or χ_f^0, to the $k = (2,2,0)$ mode only, then we would just have two additional parameters, $\{\delta\omega_0^{(0)}, \delta\tau_0^{(0)}\}$. In this paper, we will restrict ourselves to corrections to the $n = 0$ and $n = 1$ terms, i.e., leading and next-to-leading order corrections to the spin, χ_f.

Using this parameterized waveform model, which we will call pSEOBNR in this paper, we infer bounds on our beyond-GR parameters for specific cases of modified gravity theories outlined in Sec. II. We detail these results in Sec. V. [HS: Should we call this waveform differently to distinguish it from your previous papers?]

C. From theory-agnostic to theory-specific QNM results

Let us now establish the connection between theory-agnostic framework of the pSEOBNR waveform model and the theory-specific QNM calculations. We begin by rewriting ω_k and τ_k, given by Eqs. (3.2) as,

$$M\omega_k = \gamma\left(\delta\omega^{(0)}\omega^{(0)} + \chi\delta\omega^{(1)}\omega^{(1)}\right) + \sum_{n=0}^{N_{\rm max}} \chi^j\omega^j\,, \tag{3.10a}$$

$$\tau_k/M = \gamma\left(\delta\tau^{(0)}\tau^{(0)} + \chi\delta\tau^{(1)}\tau^{(1)}\right) + \sum_{n=0}^{N_{\rm max}} \chi^{(n)}\tau^{(n)}\,, \tag{3.10b}$$

We will work exclusively with the $\ell = m = 2$ and $n = 0$ (fundamental mode) QNM, i.e., $k = \{2, 2, 0\}$. For this reason we will omit the subcripts k hereafter and no ambiguity in notation between the overtone index and the subscript n in the series should arise. We have also pulled out from the sum all beyond-GR corrections, restricting ourselves to the nonspinning ($n = 0$) and linear-order in spin ($n = 1$) corrections to the Kerr QNMs.

How can we determine the beyond-GR corrections? In GR, comparison between the numerically determined Kerr QNMs against the fitting formula (3.10) fixes the GR expansion coefficients $\omega^{(n)}$, $\tau^{(n)}$. We can proceed in a similar way with

[1] Note that we use l to denote the angular dependence index and ℓ to denote the coupling constant in Sec. III A.

[2] This waveform model is available in LALSuite [35] as the SEOBNRv4HM_PA waveform approximant.

Theory	p	$\delta\omega^{(0)}_{220}$	$\delta\tau^{(0)}_{220}$	$\delta\omega^{(1)}_{220}$	$\delta\tau^{(1)}_{220}$	Ref.
EdGB	4	0.0107	0.0044	−0.2480	−1.101	[46, 47]
dCS	4	3.1964	6.3619	41.199	794.66	[21]
cubic EFT	4	−0.5813	2.6469	−3.8620	265.12	[23]
quartic EFT	6	−0.2114	−0.6070	−1.5263	171.35	[23]

TABLE II. Summary of theory-specific QNM calculations. We summarize each theory we have considered together with: the exponent p at which their QNM-modification enters, the corresponding modifications to the oscillation frequency $\delta\omega^{(n)}_{220}$ and decay time $\delta\tau^{(n)}_{220}$, and the references from which we used the results from.

QNMs calculated in the context of a beyond-GR theory. In particular, in the literature, we can already find fitting formulas relating the QNMs to the BHs mass, spin and coupling constant ℓ, the latter being specific to each theory, up to $n = 1$ in the spin expansion (see Table II). The idea is then to compare these formulas against Eq. (3.10) to fix p, $\delta\omega^{(n)}$, and $\delta\tau^{(n)}$.

This means that using the `pSEOBNR` waveform model with theory-specific informed QNMs we reduce the parameter space of beyond-GR parameters to ℓ alone. We emphasize that our procedure is different from that of Ref. [27] which, for a given value of p, varied all ℓ, $\delta\omega^{(n)}$ and $\delta\tau^{(n)}$ parameters.

As we have seen in Sec. II, the QNM of slowly-rotating BHs is modified gravity theories come in two families depending on their transformation upon a parity transformation: axial and polar. Which is the one we use to match against Eqs. (3.10)? To answer this question one has to work with a chosen theory and perform a translation between the metric perturbations $h_{\mu\nu}$ in the Regger-Wheeler-Zerilli gauge [42, 43] and connect it with the transverse-traceless gauge used to described GWs (see e.g. Ref. [44], Sec. xxx), In GR, both axial and polar QNMs are the same (a property known as *isospectrality*) and therefore which QNM we use to model the ringdown makes no difference. In beyond-GR theories, isospectrality is in general broken (see the discussion in Ref. [45] for a counterexample). Thus, how axial and polar gravitational QNMs appear in the GW signal has to be answered on theory-by-theory basis. This is outside the scope of this paper and here we take the more pragmatic approach of simply choosing the *least damped gravitational mode between the two parities.* The justification is this is the mode (if excited during the merger) which is the most likely to appear in the signal.

We performed the mapping between theory-specific QNM calculation and the ParSpec framework under the hypothesis above for the theories listed in Sec. II. We summarize our result in Table II and leave the details of our calculations to Appendix A.

In Fig. 1 we show an illustrative waveform for GR (solid line; using the `SEOBNR` model) and in the cubic EFT of gravity (dashed line; using the `pSEOBNR` model), including the leading-order $n = 0$ deformations to the fundamental QNM (see Table II). We chose binary parameters similar to GW150914, consisting of a quasicircular, nonspinning binary with detector-frame masses $m_1^{\rm dec} = 39\ {\rm M}_\odot$ and $m_2^{\rm dec} = 31\ {\rm M}_\odot$. The top panel shows the + polarization of the GW h_+ in both theories, while the bottom panel shows the amplitude $|h| = (h_+^2 + h_\times^2)^{1/2}$ and instantaneous frequency f, all as functions of time t. The signal

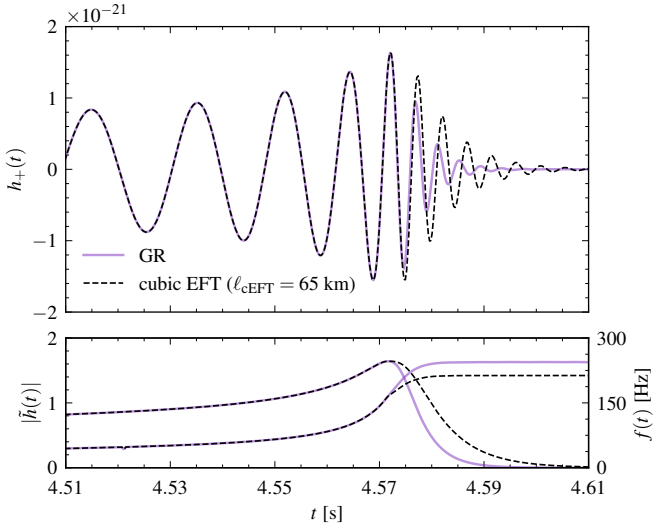

FIG. 1. (Color online). Example GW signal with GW1509140-like parameters for both GR (solid line) and cubic EFT of GR (dashed line) with the leading-order $n = 0$ modifications to the fundamental QNM, for $\ell_{\rm cEFT} = 65$ km. The former is computed with the `SEOBNR` model, while the latter with the `pSEOBNR` model, with ringdown modifications according to the results in Table II. Top panel: the + polarization $h_+(t)$. Bottom panel: the GW amplitude $|\tilde{h}(t)|$ (left axes) and the instantaneous frequency $f(t)$ (right axes).

are identical up to the merger, after which they differ during the ringdown. By construction, the ringdown is lasts longer for the cubic EFT of GR waveform and with a smaller instantaneous frequency (see the bottom panel) due to the negative value of the $\delta\omega^{(0)}$ coefficient in this theory.

IV. PARAMETER INFERENCE

In this section, we provide a basic outline of the Bayesian formalism we use to infer the properties of the underlying GW signal, identify the most promising events from the catalog of GW observations to base our analyses on, and discuss the key insights they provide in constraining predictions of modified gravity theories.

A. Bayesian formalism

If we assume that a GW signal observed in detector data d is accurately described by our waveform model `pSEOBNR`, we can infer the parameters of the model, $\boldsymbol{\lambda}$, given the hypothesis $\mathcal{H}$, using Bayes' theorem,

$$P(\boldsymbol{\lambda}|d,\mathcal{H}) = \frac{p(\boldsymbol{\lambda}|\mathcal{H})\,\mathcal{L}(d|\boldsymbol{\lambda},\mathcal{H})}{E(d|\mathcal{H})}\,, \tag{4.1}$$

where $P(\boldsymbol{\lambda}|d,\mathcal{H})$ is the posterior probability distribution, $p(\boldsymbol{\lambda}|\mathcal{H})$ the prior, $\mathcal{L}(d|\boldsymbol{\lambda},\mathcal{H})$ the likelihood, and $E(d|\mathcal{H})$ the evidence. The set of parameters, $\boldsymbol{\lambda}$ is a union of the GR waveform model parameters $\boldsymbol{\theta}$ (c.f. Sec. III B), and ℓ, the only non-GR

parameter in this problem which, we recall, set the characteristic length-scale in which deviations from GR become relevant in each of the theories described in Sec. II. Hence,

$$\boldsymbol{\lambda} = \{\ell\} \cup \{\boldsymbol{\theta}\}. \tag{4.2}$$

Assuming stationary Gaussian noise, we can write the (log) likelihood function as,

$$\ln \mathcal{L}(d|\boldsymbol{\lambda}, \mathcal{H}) \propto -\tfrac{1}{2}\langle d - h(\boldsymbol{\lambda})|d - h(\boldsymbol{\lambda})\rangle\,, \tag{4.3}$$

with noise-weighted inner product $\langle\cdot|\cdot\rangle$ defined as,

$$\langle A|B\rangle = \int_{f_{\rm low}}^{f_{\rm high}} \mathrm{d}f\, \frac{\tilde{A}^*(f)\tilde{B}(f) + \tilde{A}(f)\tilde{B}^*(f)}{S_n(f)}\,, \tag{4.4}$$

where $\tilde{A}(f)$ is the Fourier transform of $A(t)$, the asterisk denotes complex conjugation and $S_n(f)$ is the power spectrum density of the detector. Assuming a specific prior distribution for our parameters (discussed further in the subsequent section), we stochastically sample over the parameter space using a Markov-Chain Monte Carlo algorithm as implemented in `LALInferenceMCMC` [48, 49], a package part of the `LALInference` software suite [35, 50]. We subsequently marginalize over the remaining parameters to obtain the posterior probability distribution function (PDF) on ℓ, i.e., $P_j(\ell|d_j, \mathcal{H})$, our main parameter of interest.

For N independent GW observations $\{d_j\}$, $j = 1, ..., N$, each characterised by a posterior probability distribution $P_j(\ell|d_j, \mathcal{H})$, the joint posterior can be written as:

$$P(\ell|\{d_j\}) = p(\ell) \prod_{j=1}^{N} \frac{P_j(\ell|d_j)}{p_j(\ell)}\,. \tag{4.5}$$

where $p_j(\ell)$ are the priors used for each observation, and $p(\ell)$ is an overall prior. Since we assume a uniform prior on ℓ, the joint posterior is identically equal to the joint likelihood. In some cases, we found it necessary to work with different prior ranges across different events, within the context of a given theory. In this situation, when combining the posteriors we use chose as our overall prior the widest one among the individual events.

B. Priors

The prior probability distribution functions on the GR parameters are assumed to be uniform over the component masses, (m_1, m_2), isotropically distributed on a sphere in the sky for the source location with $p(d_L) \propto d_L^2$, and isotropic on the binary orientation, $p(\iota, \psi, \phi_0) \propto \sin\iota$. For the spins (χ_1, χ_2), we assume a prior uniform and isotropic in the spin magnitudes and restrict ourselves to the z-components. This spin-prior choice can be specified in `LALInference` using the option `alignedspin-zprior`. The prior on t_0 is uniform and its range is informed by our detection pipelines.

Among our beyond-GR parameters, $\{\ell, \delta\omega_k^{(n)}\delta\tau_k^{(n)}\}$, as already mentioned in the previous section, we hold $\{\delta\omega_k^{(n)}\}$ and $\{\delta\tau_k^{(n)}\}$ fixed to theory-specific predictions, and allow only ℓ to freely vary. For such cases, we assume a prior uniform between appropriate ranges on ℓ, making sure that our marginalized posterior distributions on ℓ do not rail over the maximum prior value on ℓ.

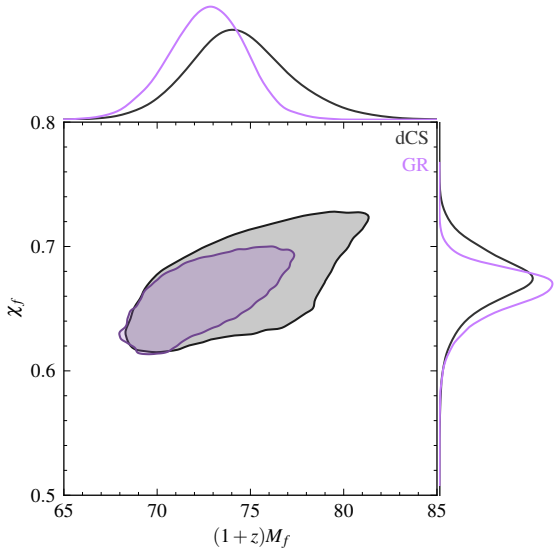

FIG. 2. (Color online). Corner plot showing that the inferred final spin χ_f, detector-frame remnant mass $(1+z)\,M_f$ for GW150915, using the same waveform model, but without (blue contours) and with the non-GR parameters different from zero (orange contours, for dCS gravity and $j = 0$). The contours represent 90% credible regions. We see that the introduction of the non-GR parameters does not bias the inference on the source parameters.

C. Event selection

The `pSEOBNR` model, as described in Sec. III B, is an *IMR* model which infers the properties of the underlying GW signal, including (independently) its ringdown properties, using the Bayesian formalism above. Naturally, the most promising candidates for our analyses are high-mass *and* loud GW observations with a significant signal-to-noise ratio (SNR) in the post-merger part of the signal. The latest LVK GW catalog [51] reported 90 observed signals not all of which are relevant for a BH ringdown analysis. In fact, in an accompanying paper [52], the pSEOBNRv4HM analysis[1], which is most similar to the `pSEOBNR` model presented in this paper, identified two events which provided the strongest bounds on measurements of the dominant (220) QNM – GW150914 [53] and GW200129 [51]. These two events, with a total mass of $XXM_\odot$ and $XXM_\odot$ respectively, are extremely similar in their source properties. These are also two of the loudest BBH signals observed to date with a total network SNR of XX and

[1] See, in particular, Sec.VIII A.2 in [52]

XX respectively. Moreover, and what is more relevant for our analysis, is their post-inspiral (merger-ringdown) SNRs, which at XX and XX respectively (see the columns for $\rho_{\text{post-insp}}$ in Table III of [54] and Table IV of [52]). In this paper, we are going to focus on these two GW events as our probes of the BH ringdown in modified theories of gravity.

The parameter inference in this paper follows configurations identical to the ones used on these events for the pSEOBNRv4HM analysis in Ref. [52]. GW150914 was a 2-detector event (HL) while GW200129 was 3-detector (HLV). We consequently use the same strain data $h(t)$, detector power-spectral-densities $S_n(f)$ and calibration envelopes as were used for the analyses in Ref. [52]. The only difference between the sampling configurations is that we do not sample over the fractional deviations in the (220) QNM frequencies and damping times, but instead on ℓ while holding $\{\delta\omega_k^{(j)}\}$, and $\{\delta\tau_k^{(j)}\}$ fixed to theory-specific predictions. In the section to follow, we enumerate through the different theories and outline the highlight results. Whenever possible, we also combine results from multiple events to obtain the strongest possible bound on ℓ.

As a first test ... [HS: Move to an appendix.]

D. General remarks on the interpretation of our results

There are two conditions that we must take into account before we can confidently claim to have placed a constraint, within our model's assumptions, with our parameter estimation study.

First, as we explained in Sec. II, all theories that we consider must be considered as an effective field theory, meaning it should be considered valid only below an energy scale, or equivalently, a length scale. As a cut-off length scale for the validity of the EFT we use,

$$\Lambda_{\text{EFT}}(\varepsilon, \mathfrak{m}) = \varepsilon G\mathfrak{m}/c^2\,, \tag{4.6}$$

where ε is a dimensionless number and $\mathfrak{m}$ is the median value of one of the mass scales involved in the problem. We also momentarily restored factors of c and G to emphasize that Λ_{EFT} has dimensions of length and hence can be compared to the coupling strength ℓ. In Refs. [1, 9, 10], $\varepsilon = 1/2$ was used, but here we consider $\varepsilon \in [0, 1]$ for generality. We will say that a bound has been placed on ℓ, if most of the support of the posterior distribution function $P(\ell)$ is in the interval $[0, \Lambda_{\text{EFT}}(\varepsilon, \mathfrak{m})]$. In practice, this can be quantified through the cumulative distribution function (CDF) associated with the marginalized posterior distribution $P(\ell)$, namely

$$P(\ell \leqslant \ell_{\text{max}}) = \int_{-\infty}^{\ell_{\text{max}}} P(\ell')\,\mathrm{d}\ell'\,. \tag{4.7}$$

For instance, we will demand that for a bound with 90% credibility to be meaningfully placed on ℓ that

$$P(\ell \leqslant \Lambda_{\text{EFT}}) \leqslant 0.9\,, \quad \text{(EFT bound)}, \tag{4.8}$$

where we let $\ell_{\text{max}} = \Lambda_{\text{EFT}}$ in Eq. (4.7), and likewise for other credibility percentiles.

Second, as already emphasized in Ref. [26], the ParSpec formalism is by construction perturbative. This means that the non-GR deformation parameters are small, that is,

$$\gamma\,\delta\omega^{(n)} \ll 1\,, \text{ and } \gamma\,\delta\tau^{(n)} \ll 1\,, \quad \text{(ParSpec bound)}, \tag{4.9}$$

for all orders n in the expansion in dimensionless spin χ and where γ is given by Eq. (3.3). We will also construct posterior distributions for these parameters and check if most of their support is concentrated to a domain with values much smaller than unity.

Another question we must consider is the following: what is the mass $\mathfrak{m}$ that we should use in Eq. (4.6)? In Refs. [1, 9, 10], which attempted to constrain dCS and shift-symmetric sGB theories with the *inspiral* part of the GW signal alone, it was natural to chose the secondary's mass m_2 as the most conservative choice, since it is (by definition) the smallest mass and hence places the lowest cut-off scale Λ_{EFT} for the validity of either of these theories as an EFT.

In our problem, the answer is not as clear. On the one hand, since we are interested in the ringdown part of the signal, it is natural to use the final mass M_f to compute Λ_{EFT}. On the other hand, one may argue that the modified gravity theory under study should be able to predict a full inspiral, merger, and ringdown of the black hole binary before we can even make such a test, and thus the same, more conservative choice $\mathfrak{m} = m_2$ should be used. Here we adopt an agnostic view to this question and consider *both* masses, m_2 and M_f, to determine Λ_{EFT}. We will then compare how different assumptions yield to different interpretations of the results of our parameter estimations.

V. RESULTS USING LIGO-VIRGO EVENTS

A. Einstein-dilaton-Gauss-Bonnet gravity

We start by showing our results for EdGB gravity. In Fig. 3 we show the marginalized posteriors of the coupling constant ℓ_{GB}, for GW150914 (top panel) and GW200129 (middle panel), with and without the spin corrections to the $(2, 2, 0)$ QNM. The bottom panel panel shows the joint posterior combining both events. We see that for both events events, the $N_{\text{max}} = 0$ posteriors are characterized by a peak away from zero. This does not mean that we are inferring a deviation from GR from data. Recall that the deviations from GR in the ParSpec framework are controlled by γ, which here reads,

$$\gamma_{\text{GB}} = \left(\frac{c^2\ell_{\text{GB}}}{GM_{\text{s}}}\right)^4\,. \tag{5.1}$$

As shown in Fig. xxx, γ_{GB} does indeed have a posterior distribution with largest support at zero, indicating consistency between data and GR. We also observe that the inclusion of the spin corrections (i.e., curves with $N_{\text{max}} = 1$) displaces the posteriors distributions towards smaller values of ℓ_{GB}.

As we emphasized in Sec. IV D, before drawing any conclusions on the allowed values for ℓ_{GB} from our parameter estimations, we must first check whether the "EFT" (4.8) and

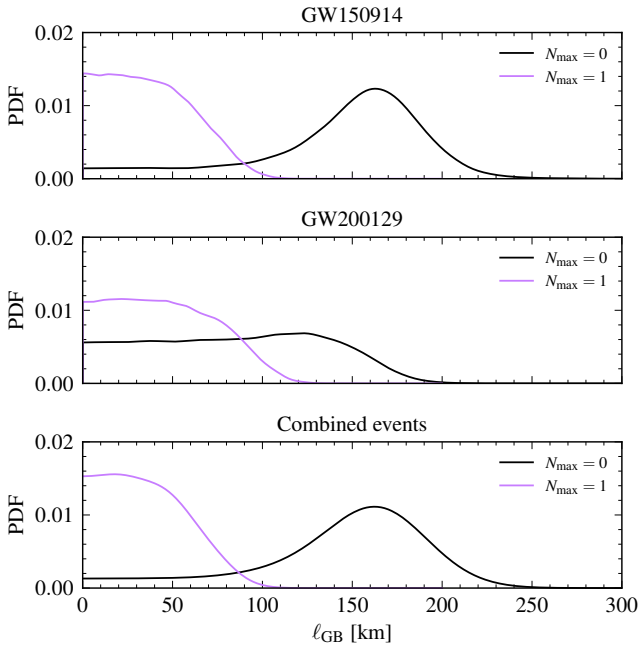

FIG. 3. (Color online). Posterior distribution function in EdGB gravity for the coupling constant $\ell_{\rm GB}$ for GW150914 (top panel), GW200129 (middle panel) and combined events (bottom panel). In all panels, different line colors correspond to the inclusion ($N_{\max} = 1$) or not ($N_{\max} = 0$) of the linear-in-spin QNM correction.

$N_{\max}$	Event	EFT bound?	ParSpec bound?	Constraint ($\mathfrak{m} = M_f$)
0	GW150914	No	Yes	–
	GW200129	No	Yes	–
	Combined	–	Yes	–
1	GW150914	No	Yes	–
	GW200129	No	Yes	–
	Combined	–	Yes	–

TABLE III. Detailed summary of our results for EdGB gravity for GW150914, GW200129, and combined events using $\mathfrak{m} = M_f$, $\varepsilon = 1/2$ and quoting only 90% credible results. We find that we cannot place any constraint on $\ell_{\rm GB}$ with our waveform model from either GW event.

"ParSpec" (4.9) bounds are satisfied. We check the validity of the EFT bound in Fig. 4. In the top (bottom) panel we show the cumulative density function of the $\ell_{\rm GB}$ posteriors for GW150914 (GW200129), obtained evaluating the integral (4.7) with $\Lambda_{\rm EFT}(\varepsilon, \mathfrak{m})$, with the mass scale set by the secondary's mass (i.e., $\mathfrak{m} = m_2$, dashed lines) or the remnant's mass ($\mathfrak{m} = M_f$, solid lines), while varying ε between 0 and 1. For GW150914, we see that for the $N_{\max} = 0$ curves, that the CDF never goes past 0.2, regardless of the mass scale $\mathfrak{m}$ used and even at $\varepsilon = 1$. This shows that that the "EFT bound" given by Eq. (4.8) is never met at a significant credibility and thus that we cannot place a bound on $\ell_{\rm GB}$. The situation is similar for GW200129 with $N_{\max} = 0$ and does not change for either event when we add spin corrections to the EdGB QNM. Altogether, *we conclude that we cannot constrain EdGB gravity with our present model*. These conclusions are summarized in Table III.

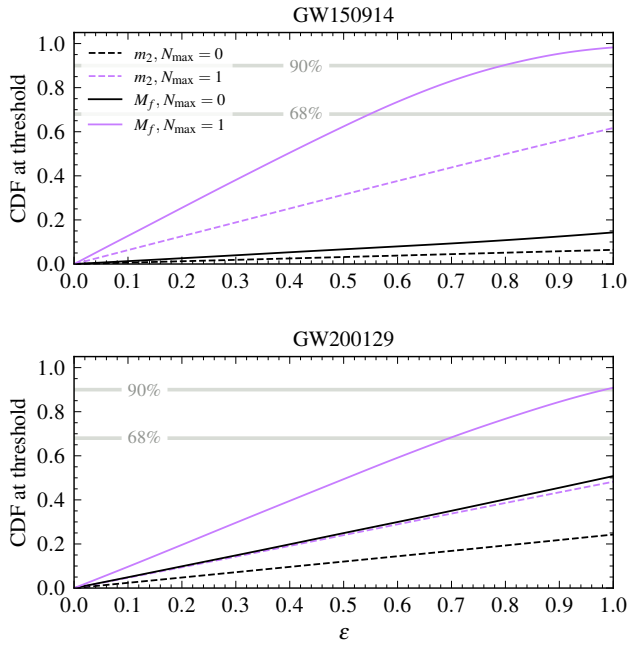

FIG. 4. (Color online). The cumulative distribution function evaluated at the cut-off $\Lambda_{\rm EFT}(\varepsilon, \mathfrak{m})$ EdGB gravity as a function of the parameter ε for both (dashed curves) $\mathfrak{m} = m_2$, the secondary's source mass, and (solid curves) $\mathfrak{m} = M_f$, the remnant's source mass, without (black curves) and with (purple curves) linear in spin QNM corrections. The horizontal lines lay at 0.68 and 0.90. We see that in no situation the curves pass through the 0.68 or 0.90 lines even at $\varepsilon = 1$. This means that no bound on $\ell_{\rm GB}$ can be placed with the events we analyzed.

Let us contrast our results with those of Ref. [1] which placed the bound $\ell_{\rm GB} \leqslant 1.33$ km using the *inspiral* portion of the neutron star-black hole binaries GW200105 and GW200115 [55] or of Refs. [9, 10], which placed the bound $\ell_{\rm GB} \leqslant 1.7$ km, by considering a selection of black hole binaries from the GWTC-1 and GWTC-1 catalogs [][1] In this cases

Based on the later, but now here confirmed, within the assumptions of our waveform model, in the case of comparable mass binaries.

Hence, here we have an example of a theory in which the inspiral portion of the signal is more constraining then the ringdown portion of the signal. As we will next, the situation is the opposite for dCS gravity.

B. Dynamical Chern-Simons

We now turn our attention to dCS gravity. In Fig. 5 we show the marginalized posterior distribution function of $\ell_{\rm CS}$ for both

[1] These bounds are, strictly speaking, valid only when the scalar field φ is small, i.e., $\varphi \ll 1$, and take into consideration only the leading-order scalar field contribution arising from the dilatonic coupling.

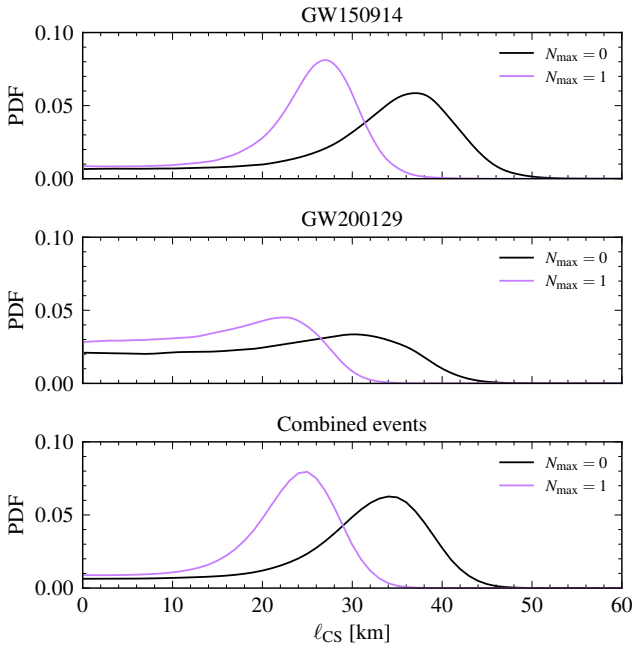

FIG. 5. (Color online). Posterior distribution function for the coupling constant $\ell_{\rm CS}$ for GW150914 (top panel), GW200129 (middle panel) and combined events (bottom panel). In all panels, we use solid and dashed lines to correspond to the inclusion or not of the linear in spin QNM correction. We stress that posteriors obtained including $j = 1$ corrections, violated conditions (4.9) and therefore should not be used to draw meaningful conclusions. We show them for illustrative purposes and also to emphasize the importance of taking conditions (4.8) and (4.9) simultaneously into consideration when analyzing the results of the parameter estimation.

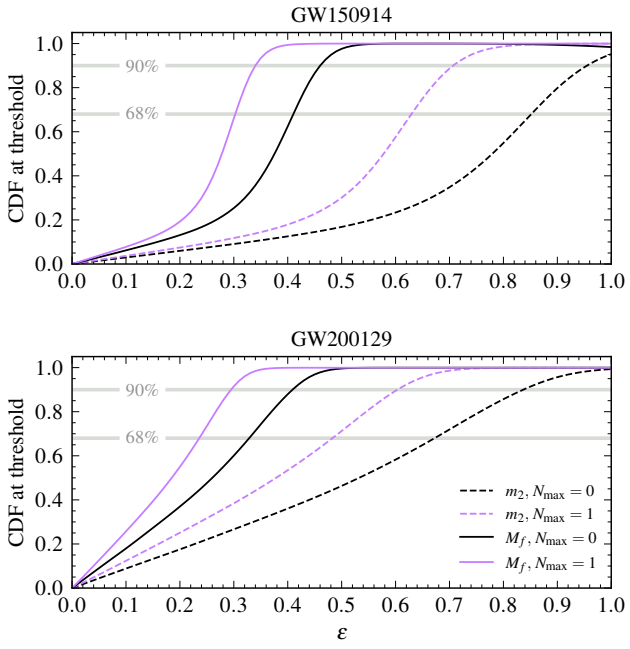

FIG. 6. (Color online). The cumulative distribution function evaluated at the cut-off $\Lambda_{\rm EFT}(\varepsilon, \mathfrak{m})$ as a function of the parameter ε for both $\mathfrak{m} = m_2$ (solid and dashed lines) and $\mathfrak{m} = M_f$ (dot-dashed and dotted lines) without (blue lines) and with (orange lines) linear-in-spin QNM corrections. The horizontal lines lay at 0.68 and 0.90. We see that the CDF curves for $\mathfrak{m} = M_f$ are above 90% for $\varepsilon = 1/2$ for both events, with and without including the $n = 1$ dCS corrections to the dominant QNM.

events GW150914 (top panel) and GW200129 (middle panel), with (dashed line) and without (solid line) spin corrections to dominant $l = m = 2$, $n = 0$ QNM. Perhaps the most salient feature of these posteriors is that they are not peaked at $\ell_{\rm CS}$, which may mislead us to believe that we are seeing a deviation from GR. This is not the case. We must remember that in the ParSpec formalism that the GR deviations are controlled by $\gamma\,\delta\omega^{(j)}$ and $\gamma\,\delta\tau^{(j)}$. We verified that these quantities do indeed peak at zero indicating consistency with GR. We also see that in both cases, that the inclusion leading-order-in-spin correction to the mode, displaces the posteriors towards smaller values of $\ell_{\rm CS}$. This can be seen more evidently by looking at the location of posterior peaks. Finally, in the bottom panel, we show the combined result for both events.

In Fig. 6 we show the cumulative distribution function (CDF) as evaluates with Eq. (4.7), with $\ell_{\max} = \Lambda_{\rm EFT}$, for both GW150914 (top panel) and GW200129 (bottom panel), where $\Lambda_{\rm EFT}$ is calculated with either $\mathfrak{m} = m_2$ (blue curves) or M_f (orange curves), and with $\varepsilon \in [0,\ 1]$. For GW150914, we see that with $\mathfrak{m} = m_2$ that Eq. (4.8) is not satisfied unless $\varepsilon \approx 0.9$ (with only $j = 0$ corrections) and $\varepsilon \approx 0.7$ (with both $j = 0$ and 1 corrections). The situation is different if we use $\mathfrak{m} = M_f$. In this case, we find that with or without spin corrections that Eq. (4.8) can be satisfied with $\varepsilon \leqslant 1/2$, i.e., below the criteria used Refs. [1, 9, 10]. This means that with our model's assumptions and using the remnant's source mass M_f to set the cut-off scale that we can claim an upper bound

$$\ell_{\rm CS} \leqslant 42.6\ {\rm km} \quad (90\%\ {\rm credibility}), \tag{5.2}$$

on dCS gravity and would constitute the first bound on this theory with gravitational-wave observations alone. We also note that since the CDF grows fast in approximate domain $\varepsilon = [0.2, 0.4]$, that a stronger, albeit at lower credibility,

$$\ell_{\rm CS} \leqslant 37.4\ {\rm km} \quad {\rm at}\ 68\%\ {\rm credibility}, \tag{5.3}$$

can also be placed, when $N_{\max} = 0$.

We can draw qualitatively similar conclusions from the GW200129 event. In particular, we find,

$$\ell_{\rm CS} \leqslant 36.6\ {\rm km} \quad (90\%\ {\rm credibility}), \tag{5.4}$$

and

$$\ell_{\rm CS} \leqslant 29.1\ {\rm km} \quad (68\%\ {\rm credibility}), \tag{5.5}$$

when $N_{\max} = 0$. These stronger bound are a consequence of the larger support for $\ell_{\rm CS} \lessapprox 15$ km for GW200129 (compare the top and middle panels in Fig. 5), and in part due to the smaller median remnant ($M_f \approx 59.5\ {\rm M}_\odot$ versus $M_f \approx 61.8\ {\rm M}_\odot$ for GW150914).

We also found for both GW events, that the perturbative-conditions (4.9) required by the ParSpec formalism is violated

for the $\gamma_{\rm CS}\,\delta\tau^{(1)}$ coefficient. This means that we cannot use these posterior to infer any meaningful bound on dCS gravity and that is why we quoted only the $N_{\rm max}=0$ bound above.

Finally, since both event individually led to a bound on $\ell_{\rm CS}$ (assuming a cut-off scale for $\mathfrak{m}=M_f$ and $j=0$), we can combine the posteriors to obtain the cumulative bound,

$$\ell_{\rm CS}\leqslant 38.7\ {\rm km}\quad (90\%\ {\rm credibility}), \tag{5.6}$$

which is the main result of this section. This bound is approximately a factor of four weaker than that placed by Ref. [2], but (i) relies only on GW observations and (ii) suggests that a ringdown analysis can potentially place constraints on theories which evade GW tests using inspiral information alone, such as the case of dCS gravity [1, 9, 10]. In Table IV we summarize our findings of this section.

$N_{\rm max}$	Event	EFT bound?	ParSpec bound?	Constraint ($\mathfrak{m}=M_f$)
0	GW150914	Yes	Yes	$\ell_{\rm CS}\leqslant 41.9$ km
	GW200129	Yes	Yes	$\ell_{\rm CS}\leqslant 35.8$ km
	Combined			$\ell_{\rm CS}\leqslant 38.7$ km
1	GW150914	Yes	No	–
	GW200129	Yes	No	–
	Combined			–

TABLE IV. Detailed summary of our results for dCS gravity for GW150914, GW200129, and combined events using $\mathfrak{m}=M_f$, $\varepsilon=1/2$ and quoting only 90% credible results. We found that while our posteriors satisfy the condition (4.8) (with $\varepsilon=1/2$), they do not obey the condition (4.9) for $j=1$. This means that our results for $N_{\rm max}=0$ are the only ones we can confidently quote. The combined bound, which is also quoted in Table II, is $\ell_{\rm CS}\leqslant 38.7$ km.

C. cubic effective-field-theory of general relativity

$N_{\rm max}$	Event	EFT bound?	ParSpec bound?	Constraint ($\mathfrak{m}=M_f$)
0	GW150914	Yes	Yes	$\ell_{\rm cEFT}\leqslant 38.2$ km
	GW200129	Yes	Yes	$\ell_{\rm cEFT}\leqslant 42.5$ km
	Combined			$\ell_{\rm cEFT}\leqslant 38.2$ km
1	GW150914	Yes	No	–
	GW200129	Yes	No	–
	Combined			–

TABLE V. Detailed summary of our results the cubic EFT of GR for GW150914, GW200129, and combined events using $\mathfrak{m}=M_f$, $\varepsilon=1/2$ and quoting only 90% credible results.

D. quartic effective-field-theory of general relativity

VI. CONCLUSIONS

We presented an unified framework to combine the parametrized formalism introduced to model deviations to

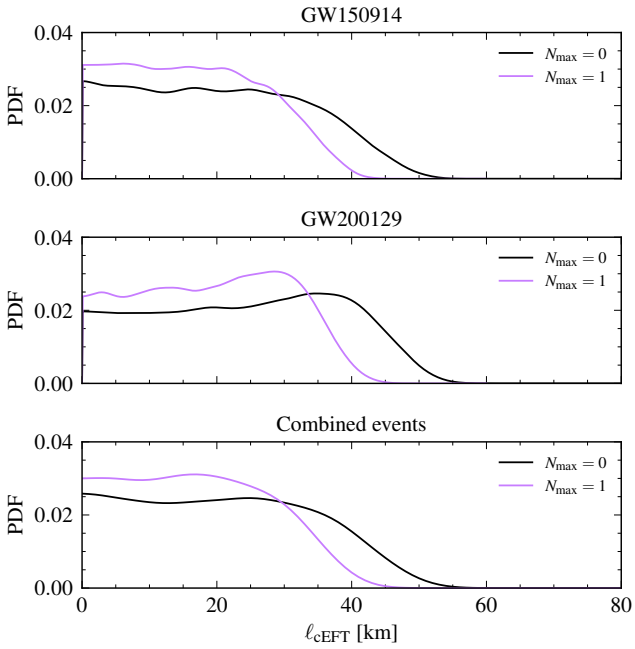

FIG. 7. (Color online). Posterior distribution function for the coupling constant $\ell_{\rm cEFT}$ for GW150914 (top panel), GW200129 (middle panel) and combined events (bottom panel). In all panels, we use solid and dashed lines to correspond to the inclusion or not of the linear in spin QNM correction. [HS: TODO]

$N_{\rm max}$	Event	EFT bound?	ParSpec bound?	Constraint ($\mathfrak{m}=M_f$)
0	GW150914	Yes	Yes	$\ell_{\rm qEFT}\leqslant 51.7$ km
	GW200129	Yes	Yes	$\ell_{\rm qEFT}\leqslant 54.8$ km
	Combined			$\ell_{\rm qEFT}\leqslant 51.3$ km
1	GW150914			
	GW200129			
	Combined			

TABLE VI. Detailed summary of our results the quartic EFT of GR for GW150914, GW200129, and combined events using $\mathfrak{m}=M_f$, $\varepsilon=1/2$ and quoting only 90% credible results. [HS: Need to debug $N_{\rm max}=1$ runs.]

the GR QNMs [26] with the `pSEOBNR` waveform model. We showed through concrete examples how theory-specific calculations QNM of slowly-rotating BHs in modified gravity theories can be mapped upon the theory-agnostic beyond-GR parameters of the ParSpec formalism. Together this allowed us to apply the `pSEOBNR` waveform model to test four modified gravity theories (EdGB, dCS, cubic, and quartic effective-field-theories of GR) using data from the GW events GW150914 and GW200129. We found, in particular that, within the assumptions of our model and by stacking posteriors, that the coupling constant of dCS gravity is bound to $\ell_{\rm CS}\leqslant 34.5$ km. In contrast, we could place any constraint of the coupling constants in EdGB gravity $\ell_{\rm GB}$. This dichotomy between these theories has an analogy with works that considered the inspiral part of the GW signal alone. In that case, it is dCS which is unconstrained, while EdGB, in principle can be constrained,

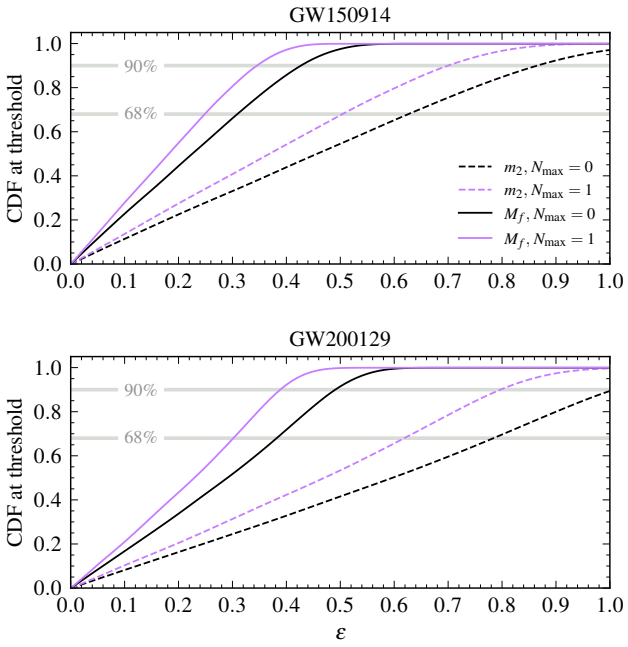

FIG. 8.

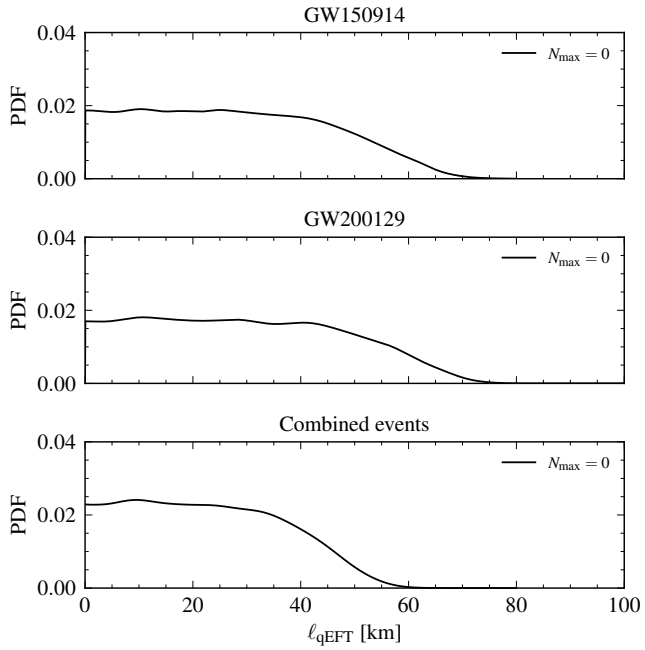

FIG. 9. (Color online). Posterior distribution function for the coupling constant $\ell_{\rm qEFT}$ for GW150914 (top panel), GW200129 (middle panel) and combined events (bottom panel). In all panels, we use solid and dashed lines to correspond to the inclusion or not of the linear in spin QNM correction. [HS: TODO]

based on results for the closely related shift-symmetric version of this theory.

Our work shows that there are theories of gravity (such as dCS) which can by-pass observational constraints from the inspiral phase alone, *yet* would not, if we analyze the ringdown. We hope that our result thus serve as additional motivation for future work modeling the late-inspiral, merger and ringdown of coalescing BHs in modified gravity theories.

Let us discuss some avenues for future work ...

[HS: TODO: say that we could try to expand the waveform model to include modification to the inspiral part too; maybe through FTI [56]?]

[HS: TODO: add that we could try to parametrize the final black hole mass and spin estimates formulas we use at the moment [39]. Maybe comment that a possible first attempt could follow [57], as done in [58, 59]. Say that ultimately we will need to informed by NR in beyond-GR.]

[HS: I suspect that by construction the $N_{\max} = 1$ cases will often fail to satisfy our perturbative bounds. If so, add explanation here.]

Appendix A: Details of the determination of the theory-specific ParSpec coefficients

1. Einstein-dilaton-Gauss-Bonnet

2. dynamical Chern-Simons

In Ref. [21] the QNMs of slow-rotating BHs in dCS gravity were calculated and it was found that the axial gravitational modes have their damping time increased as we increase the Chern-Simons coupling $\ell_{\rm CS}$ at fixed spin χ of the BH. Hence, according to the prescription of Sec. III C, this is the branch of QNMs we will select.

We can now proceed to determine $\delta\omega^{(n)}$ and $\delta\tau^{(n)}$ as follows. Using the fitting formula Eq. (54a) of [21], namely,

$$M\omega_{\rm CS} = c_1 + c_2\kappa\zeta + (c_3 + c_4\kappa\zeta)\,(1-\chi)^{c_5+c_6\kappa\zeta}, \qquad \text{(A1)}$$

and similarly for the imaginary part $\mathrm{Im}(\sigma_{\rm CS}) = -1/\tau_{\rm CS}$. Here $\kappa = 1/(16\pi)$, $\zeta = \ell_{\rm CS}^4/(M^4\kappa)$, and thus

$$\kappa\zeta = (\ell_{\rm CS}/M)^4\,, \qquad \text{(A2)}$$

and c_i are fitting coefficients which can be found in Ref. [21], Table II. In the context of a binary BH merger, M is interpreted as the remnant mass M_f.

We now expand Eq. (A1) to leading-orders in χ and $\ell_{\rm CS}$, and gather the terms proportional to $\ell_{\rm CS}$. We obtain

$$M_f\,\omega_{\rm CS} = \left[0.3722 + 1.1945(\ell_{\rm CS}/M_f)^4\right] + \left[0.1861 + 5.1828(\ell_{\rm CS}/M_f)^4\right]\chi\,, \qquad \text{(A3)}$$

where we made use of the numerical value of the coefficients c_i. We find that (reassuringly) that the nonrotating GR part of the expression above agree with $\omega^{(0)}$ of Ref. [26] to 0.5% relative percent error. The same error estimate is larger ($\approx 20\%$) for the linear-in-spin coefficient; 0.1861 in comparison to 0.1258 of Ref. [26]. We attribute this difference to Ref. [21] having fitted Eq. (A1) to QNM data compute to linear-order in spin, whereas [26] fitted Eq. (3.2) to Kerr QNM valid to all orders in spin.

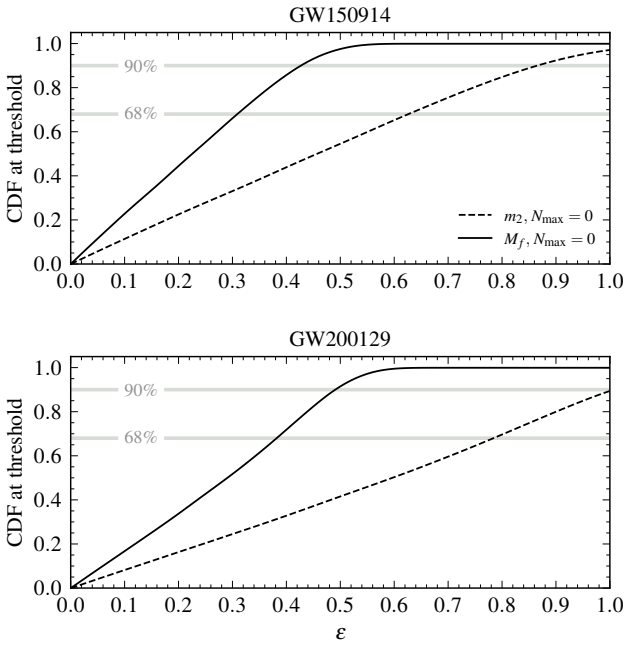

FIG. 10.

We can now isolate the dCS corrections from Eq. (A3) and compare against Eq. (3.10), to find

$$p_{\rm CS} = 4\,, \quad \delta\omega^{(0)}_{\rm CS} = 3.1964\,, \quad \delta\omega^{(1)}_{\rm CS} = 41.199\,. \tag{A4}$$

We can carry the same steps for $\tau_{\rm CS}$ and find

$$\delta\tau^{(0)}_{\rm CS} = 6.3619\,, \quad \delta\tau^{(1)}_{\rm CS} = 794.66\,. \tag{A5}$$

which completes the set of fixed parameters beyond-GR parameters in the ringdown of the `pSEOBNR` waveform model. We remark that the alarmingly large values of $\delta\omega^{(1)}_{\rm CS}$ and $\delta\tau^{(1)}_{\rm CS}$ are compensated by the assumptions that $(\ell_{\rm CS}/M_f)^2$ and χ are much less than unity. These are the assumptions use to calculate the QNM frequencies both in Ref. [21].

3. Effective-field-theories GR

ACKNOWLEDGEMENTS

We thank Emanuele Berti, Andrea Maselli, Caio F. B. Macedo, Deyan Mihaylov, Serguei Ossokine, Scott E. Perkins, and Helvi Witek for discussions. We are grateful for the computational resources provided by the Max Planck Institute for Gravitational Physics in Potsdam, specifically the high-performace computing cluster Hypatia and to Steffen Grunewald for assistance. The authors would like to thank everyone at the frontline of the Covid-19 pandemic.

[1] Z. Lyu, N. Jiang, and K. Yagi, "Constraints on Einstein-dilation-Gauss-Bonnet gravity from black hole-neutron star gravitational wave events," Phys. Rev. D **105**, 064001 (2022), arXiv:2201.02543 [gr-qc].

[2] H. O. Silva, A. M. Holgado, A. Cárdenas-Avendaño, and N. Yunes, "Astrophysical and theoretical physics implications from multimessenger neutron star observations," Phys. Rev. Lett. **126**, 181101 (2021), arXiv:2004.01253 [gr-qc].

[3] N. Sennett, R. Brito, A. Buonanno, V. Gorbenko, and L. Senatore, "Gravitational-Wave Constraints on an Effective Field-Theory Extension of General Relativity," Phys. Rev. D **102**, 044056 (2020), arXiv:1912.09917 [gr-qc].

[4] D. D. Doneva and S. S. Yazadjiev, "New Gauss-Bonnet Black Holes with Curvature-Induced Scalarization in Extended Scalar-Tensor Theories," Phys. Rev. Lett. **120**, 131103 (2018), arXiv:1711.01187 [gr-qc].

[5] H. O. Silva, J. Sakstein, L. Gualtieri, T. P. Sotiriou, and E. Berti, "Spontaneous scalarization of black holes and compact stars from a Gauss-Bonnet coupling," Phys. Rev. Lett. **120**, 131104 (2018), arXiv:1711.02080 [gr-qc].

[6] A. Dima, E. Barausse, N. Franchini, and T. P. Sotiriou, "Spin-induced black hole spontaneous scalarization," Phys. Rev. Lett. **125**, 231101 (2020), arXiv:2006.03095 [gr-qc].

[7] C. A. R. Herdeiro, E. Radu, H. O. Silva, T. P. Sotiriou, and N. Yunes, "Spin-induced scalarized black holes," Phys. Rev. Lett. **126**, 011103 (2021), arXiv:2009.03904 [gr-qc].

[8] E. Berti, L. G. Collodel, B. Kleihaus, and J. Kunz, "Spin-induced black-hole scalarization in Einstein-scalar-Gauss-Bonnet theory," Phys. Rev. Lett. **126**, 011104 (2021), arXiv:2009.03905 [gr-qc].

[9] R. Nair, S. Perkins, H. O. Silva, and N. Yunes, "Fundamental Physics Implications for Higher-Curvature Theories from Binary Black Hole Signals in the LIGO-Virgo Catalog GWTC-1," Phys. Rev. Lett. **123**, 191101 (2019), arXiv:1905.00870 [gr-qc].

[10] S. E. Perkins, R. Nair, H. O. Silva, and N. Yunes, "Improved gravitational-wave constraints on higher-order curvature theories of gravity," Phys. Rev. D **104**, 024060 (2021), arXiv:2104.11189 [gr-qc].

[11] N. Yunes and F. Pretorius, "Dynamical Chern-Simons Modified Gravity. I. Spinning Black Holes in the Slow-Rotation Approximation," Phys. Rev. D **79**, 084043 (2009), arXiv:0902.4669 [gr-qc].

[12] K. Konno, T. Matsuyama, and S. Tanda, "Rotating black hole in extended Chern-Simons modified gravity," Prog. Theor. Phys. **122**, 561–568 (2009), arXiv:0902.4767 [gr-qc].

[13] A. N. Lommen, A. Zepka, D. C. Backer, M. McLaughlin, J. C. Cordes, Z. Arzoumanian, and K. Xilouris, "New pulsars from an arecibo drift scan search," Astrophys. J. **545**, 1007 (2000), arXiv:astro-ph/0008054.

[14] Z. Arzoumanian *et al.* (NANOGrav), "The NANOGrav 11-year Data Set: High-precision timing of 45 Millisecond Pulsars," Astrophys. J. Suppl. **235**, 37 (2018), arXiv:1801.01837 [astro-ph.HE].

[15] T. E. Riley *et al.*, "A NICER View of PSR J0030+0451: Millisecond Pulsar Parameter Estimation," Astrophys. J. Lett. **887**, L21 (2019), arXiv:1912.05702 [astro-ph.HE].

[16] M. C. Miller *et al.*, "PSR J0030+0451 Mass and Radius from NICER Data and Implications for the Properties of Neutron Star Matter," Astrophys. J. Lett. **887**, L24 (2019), arXiv:1912.05705 [astro-ph.HE].

[17] B. P. Abbott *et al.* (LIGO Scientific, Virgo), "GW170817: Observation of Gravitational Waves from a Binary Neutron Star Inspiral," Phys. Rev. Lett. **119**, 161101 (2017), arXiv:1710.05832 [gr-qc].

[18] N. Yunes and C. F. Sopuerta, "Perturbations of Schwarzschild Black Holes in Chern-Simons Modified Gravity," Phys. Rev. D **77**, 064007 (2008), arXiv:0712.1028 [gr-qc].

[19] V. Cardoso and L. Gualtieri, "Perturbations of Schwarzschild black holes in Dynamical Chern-Simons modified gravity," Phys. Rev. D **80**, 064008 (2009), [Erratum: Phys.Rev.D 81, 089903 (2010)], arXiv:0907.5008 [gr-qc].

[20] C. Molina, P. Pani, V. Cardoso, and L. Gualtieri, "Gravitational signature of Schwarzschild black holes in dynamical Chern-Simons gravity," Phys. Rev. D **81**, 124021 (2010), arXiv:1004.4007 [gr-qc].

[21] P. K. Wagle, N. Yunes, and H. O. Silva, "Quasinormal modes of slowly-rotating black holes in dynamical Chern-Simons gravity," (2021), arXiv:2103.09913 [gr-qc].

[22] P. A. Cano, K. Fransen, and T. Hertog, "Ringing of rotating black holes in higher-derivative gravity," Phys. Rev. D **102**, 044047 (2020), arXiv:2005.03671 [gr-qc].

[23] P. A. Cano, K. Fransen, T. Hertog, and S. Maenaut, "Gravitational ringing of rotating black holes in higher-derivative gravity," Phys. Rev. D **105**, 024064 (2022), arXiv:2110.11378 [gr-qc].

[24] C. de Rham, J. Francfort, and J. Zhang, "Black Hole Gravitational Waves in the Effective Field Theory of Gravity," Phys. Rev. D **102**, 024079 (2020), arXiv:2005.13923 [hep-th].

[25] V. Cardoso, M. Kimura, A. Maselli, and L. Senatore, "Black Holes in an Effective Field Theory Extension of General Relativity," Phys. Rev. Lett. **121**, 251105 (2018), arXiv:1808.08962 [gr-qc].

[26] A. Maselli, P. Pani, L. Gualtieri, and E. Berti, "Parametrized ringdown spin expansion coefficients: a data-analysis framework for black-hole spectroscopy with multiple events," Phys. Rev. D **101**, 024043 (2020), arXiv:1910.12893 [gr-qc].

[27] G. Carullo, "Enhancing modified gravity detection from gravitational-wave observations using the parametrized ringdown spin expansion coeffcients formalism," Phys. Rev. D **103**, 124043 (2021), arXiv:2102.05939 [gr-qc].

[28] S. Gossan, J. Veitch, and B. S. Sathyaprakash, "Bayesian model selection for testing the no-hair theorem with black hole ringdowns," Phys. Rev. D **85**, 124056 (2012), arXiv:1111.5819 [gr-qc].

[29] J. Meidam, M. Agathos, C. Van Den Broeck, J. Veitch, and B. S. Sathyaprakash, "Testing the no-hair theorem with black hole ringdowns using TIGER," Phys. Rev. D **90**, 064009 (2014), arXiv:1406.3201 [gr-qc].

[30] G. Carullo *et al.*, "Empirical tests of the black hole no-hair conjecture using gravitational-wave observations," Phys. Rev. D **98**, 104020 (2018), arXiv:1805.04760 [gr-qc].

[31] A. Krolak and B. F. Schutz, "Coalescing binaries – Probe of the universe," Gen. Rel. Grav. **19**, 1163–1171 (1987).

[32] R. Brito, A. Buonanno, and V. Raymond, "Black-hole Spectroscopy by Making Full Use of Gravitational-Wave Modeling," Phys. Rev. D **98**, 084038 (2018), arXiv:1805.00293 [gr-qc].

[33] A. Ghosh, R. Brito, and A. Buonanno, "Constraints on quasinormal-mode frequencies with LIGO-Virgo binary–black-hole observations," Phys. Rev. D **103**, 124041 (2021), arXiv:2104.01906 [gr-qc].

[34] D. P. Mihaylov, S. Ossokine, A. Buonanno, and A. Ghosh, "Fast post-adiabatic waveforms in the time domain: Applications to compact binary coalescences in LIGO and Virgo," Phys. Rev. D **104**, 124087 (2021), arXiv:2105.06983 [gr-qc].

[35] LIGO Scientific Collaboration, "LIGO Algorithm Library - LALSuite," free software (GPL) (2018).

[36] R. Cotesta, A. Buonanno, A. Bohé, A. Taracchini, I. Hinder, and S. Ossokine, "Enriching the Symphony of Gravitational Waves from Binary Black Holes by Tuning Higher Harmonics," Phys. Rev. D **98**, 084028 (2018), arXiv:1803.10701 [gr-qc].

[37] A. Bohé *et al.*, "Improved effective-one-body model of spinning, nonprecessing binary black holes for the era of gravitational-wave astrophysics with advanced detectors," Phys. Rev. D **95**, 044028 (2017), arXiv:1611.03703 [gr-qc].

[38] A. Taracchini *et al.*, "Effective-one-body model for black-hole binaries with generic mass ratios and spins," Phys. Rev. D **89**, 061502 (2014), arXiv:1311.2544 [gr-qc].

[39] F. Hofmann, E. Barausse, and L. Rezzolla, "The final spin from binary black holes in quasi-circular orbits," Astrophys. J. Lett. **825**, L19 (2016), arXiv:1605.01938 [gr-qc].

[40] E. Berti, V. Cardoso, and C. M. Will, "On gravitational-wave spectroscopy of massive black holes with the space interferometer LISA," Phys. Rev. D **73**, 064030 (2006), arXiv:gr-qc/0512160.

[41] E. Berti, V. Cardoso, and A. O. Starinets, "Quasinormal modes of black holes and black branes," Class. Quant. Grav. **26**, 163001 (2009), arXiv:0905.2975 [gr-qc].

[42] T. Regge and J. A. Wheeler, "Stability of a Schwarzschild singularity," Phys. Rev. **108**, 1063–1069 (1957).

[43] F. J. Zerilli, "Effective potential for even parity Regge-Wheeler gravitational perturbation equations," Phys. Rev. Lett. **24**, 737–738 (1970).

[44] M. Maggiore, *Gravitational Waves. Vol. 2: Astrophysics and Cosmology* (Oxford University Press, 2018).

[45] L. Hui, A. Podo, L. Santoni, and E. Trincherini, "Effective Field Theory for the perturbations of a slowly rotating black hole," JHEP **12**, 183 (2021), arXiv:2111.02072 [hep-th].

[46] J. L. Blázquez-Salcedo, C. F. B. Macedo, V. Cardoso, V. Ferrari, L. Gualtieri, F. S. Khoo, J. Kunz, and P. Pani, "Perturbed black holes in Einstein-dilaton-Gauss-Bonnet gravity: Stability, ringdown, and gravitational-wave emission," Phys. Rev. D **94**, 104024 (2016), arXiv:1609.01286 [gr-qc].

[47] L. Pierini and L. Gualtieri, "Quasi-normal modes of rotating black holes in Einstein-dilaton Gauss-Bonnet gravity: the first order in rotation," Phys. Rev. D **103**, 124017 (2021), arXiv:2103.09870 [gr-qc].

[48] C. Rover, R. Meyer, and N. Christensen, "Bayesian inference on compact binary inspiral gravitational radiation signals in interferometric data," Class. Quant. Grav. **23**, 4895–4906 (2006), arXiv:gr-qc/0602067.

[49] M. van der Sluys, V. Raymond, I. Mandel, C. Rover, N. Christensen, V. Kalogera, R. Meyer, and A. Vecchio, "Parameter estimation of spinning binary inspirals using Markov-chain Monte Carlo," Class. Quant. Grav. **25**, 184011 (2008), arXiv:0805.1689 [gr-qc].

[50] J. Veitch *et al.*, "Parameter estimation for compact binaries with ground-based gravitational-wave observations using the LALInference software library," Phys. Rev. D **91**, 042003 (2015), arXiv:1409.7215 [gr-qc].

[51] R. Abbott *et al.* (LIGO Scientific, VIRGO, KAGRA), "GWTC-3: Compact Binary Coalescences Observed by LIGO and Virgo During the Second Part of the Third Observing Run," (2021), arXiv:2111.03606 [gr-qc].

[52] R. Abbott *et al.* (LIGO Scientific, VIRGO, KAGRA), "Tests of General Relativity with GWTC-3," (2021), arXiv:2112.06861 [gr-qc].

[53] B. P. Abbott *et al.* (LIGO Scientific, Virgo), "Observation of Gravitational Waves from a Binary Black Hole Merger," Phys. Rev. Lett. **116**, 061102 (2016), arXiv:1602.03837 [gr-qc].

[54] B. P. Abbott *et al.* (LIGO Scientific, Virgo), "Tests of General Relativity with the Binary Black Hole Signals from the LIGO-Virgo Catalog GWTC-1," Phys. Rev. D **100**, 104036 (2019), arXiv:1903.04467 [gr-qc].

[55] R. Abbott *et al.* (LIGO Scientific, KAGRA, VIRGO), "Observation of Gravitational Waves from Two Neutron Star–Black Hole Coalescences," Astrophys. J. Lett. **915**, L5 (2021), arXiv:2106.15163 [astro-ph.HE].

[56] A. K. Mehta, A. Buonanno, R. Cotesta, A. Ghosh, N. Sennett, and J. Steinhoff, "Tests of General Relativity with Gravitational-Wave Observations using a Flexible–Theory-Independent Method," (2022), arXiv:2203.13937 [gr-qc].

[57] A. Buonanno, L. E. Kidder, and L. Lehner, "Estimating the final spin of a binary black hole coalescence," Phys. Rev. D **77**, 026004 (2008), arXiv:0709.3839 [astro-ph].

[58] P. Jai-akson, A. Chatrabhuti, O. Evnin, and L. Lehner, "Black hole merger estimates in Einstein-Maxwell and Einstein-Maxwell-dilaton gravity," Phys. Rev. D **96**, 044031 (2017), arXiv:1706.06519 [gr-qc].

[59] S.-L. Li, W.-D. Tan, P. Wu, and H. Yu, "Estimating the final spin of binary black holes merger in STU supergravity," Nucl. Phys. B **975**, 115665 (2022), arXiv:2003.01957 [gr-qc].